Electronic anti-Stokes–Raman emission in quantum-cascade lasers

A. Gomez-Iglesias,[a] D. Wasserman, and C. Gmachl
Department of Electrical Engineering and PRISM, Princeton University, Princeton, New Jersey 08544

A. Belyanin
Department of Physics, Texas A&M University, College Station, Texas 77843

D. L. Sivco
Bell Laboratories, Lucent Technologies, Murray Hill, New Jersey 07974

(Received 10 June 2005; accepted 27 October 2005; published online 29 December 2005)

In this letter, the observation of electronic anti-Stokes–Raman emission in quantum-cascade lasers is reported. We present two distinct active region designs with enhanced anti-Stokes–Raman nonlinearity. The pump laser is monolithically integrated with the nonlinear region in a two-stack active core within the same waveguide. Electronic Raman emission was observed in both designs. Additionally, for the design with positive detuning, an incoherent upconversion signal resulting from optical pumping is detected. © *2005 American Institute of Physics*. [DOI: 10.1063/1.2150585]

Quantum-cascade (QC) lasers[1] are semiconductor injection lasers based on optical and electronic intersubband transitions (ISTs). A QC laser is typically comprised of several tens of cascaded active region and injector pairs, each of them containing about eight to ten wells and barriers. The emission characteristics of conventional diode lasers are, to a large extent, determined by the devices' material properties, notably the materials' band gap. Light emission from intersubband transitions in QC lasers, however, can be controlled via the well and barrier thicknesses and the external applied electric field.

It is well known that ISTs in asymmetric coupled quantum wells can display giant nonlinear optical susceptibilities.[2–4] These effects result from the large optical dipole matrix elements of ISTs and the enhancement of nonlinearities occurring near resonance of these transitions. With QC lasers, it is possible to selectively replace active regions/injectors with nonlinear elements or to integrate nonlinear transitions directly into the active regions themselves, thus allowing for efficient intracavity wave mixing.[5] This was recently demonstrated for sum frequency, second harmonic, and third harmonic generation.[6–8]

The monolithic integration of resonant optical nonlinearities based on ISTs with QC lasers has several advantages. First, QC lasers can provide high optical power densities making them very effective pump sources. The emission of pump photons and the stimulation of nonlinear processes can be made to occur in every stage of the cascade. Therefore, the entire waveguide core contributes to the nonlinear generation of light. In addition, such a device design results in good overlap between pump modes and the nonlinear region.

In this context, stimulated Raman scattering has been one such subject of research. To date, only Stokes Raman lasing has been achieved in two separate experiments; one using externally pumped asymmetric quantum-well structures,[9] and the other in QC lasers with the nonlinearity integrated into the active region.[10] In both cases, the difference between pump and Raman laser frequencies was of the order of 40–50 meV. Here, we report on the observation of electronic Anti-Stokes (AS)–Raman emission in QC lasers. This is the first step toward AS–Raman lasing, which holds promise to extend straightforward operation of unstrained InP QC lasers to wavelengths below 4 μm. Implementing nonlinear effects based on Raman transitions has the added advantage that no phase matching is required.

QC lasers have been designed comprised of two monolithically integrated stacks of active regions and injectors, one stack being the pump laser and the other stack forming the AS nonlinear region (Fig. 1). Each stack is designed at an electrical field best suited for the optical transition of interest. Apportionment of the appropriate subvoltage across each stack upon the application of an external bias has previously proven to be effective,[11,12] and is a straightforward consequence of Kirchhoff's laws.

Intersubband transitions in the nonlinear region were designed so as to optimize the optical dipole matrix elements between levels 2, 3, and 4, z_{43} and z_{42}, respectively. This optimization enhances the relevant third-order nonlinearity for AS emission. Electrons in Level 3 of the nonlinear region undergo AS–Raman scattering stimulated by the pump light, emitting photons with energy $h\nu_{\mathrm{AS}}=\Delta E_{42}+\delta$, where ΔE_{42} is the energy separation between Levels 4 and 2 and δ is the detuning, defined as $\delta=h\nu_{\mathrm{pump}}-\Delta E_{43}$. Fast depletion of the lower Level (2) is obtained by tailoring ΔE_{21} close to the longitudinal optical phonon resonance.

AS–Raman emission has been observed with a variety of samples, some corresponding to designs with positive detuning, while in others pumping takes place well below resonance (negative detuning). Two designs, D3015 and D2924, demonstrating each of the former cases, are displayed in Fig. 1 and discussed in more detail below.

The lasers are processed as conventional deep-etched ridge waveguide lasers, with stripe widths ranging from 6 to 20 μm. The lasers are cleaved to 2–3 mm in length and the facets are left uncoated. Figure 2 shows the normalized mode intensity mode profile and the profile of the real part of the refractive index in the (reverse) growth direction for both the AS and pump fundamental modes in wafer D3015. The normalized mode overlap of the pump mode with the AS and pump active regions is 0.32 and 0.33, respectively. The confinement factor of the AS light is 0.38 for the nonlinear re-

[a]Present address: School of Physics and Astronomy, University of St. Andrews, Fife KY16 9SS, UK; electronic mail: agil@st-andrews.ac.uk

 © 2005 American Institute of Physics
Downloaded 29 Aug 2006 to 128.112.35.48. Redistribution subject to AIP license or copyright, see http://apl.aip.org/apl/copyright.jsp

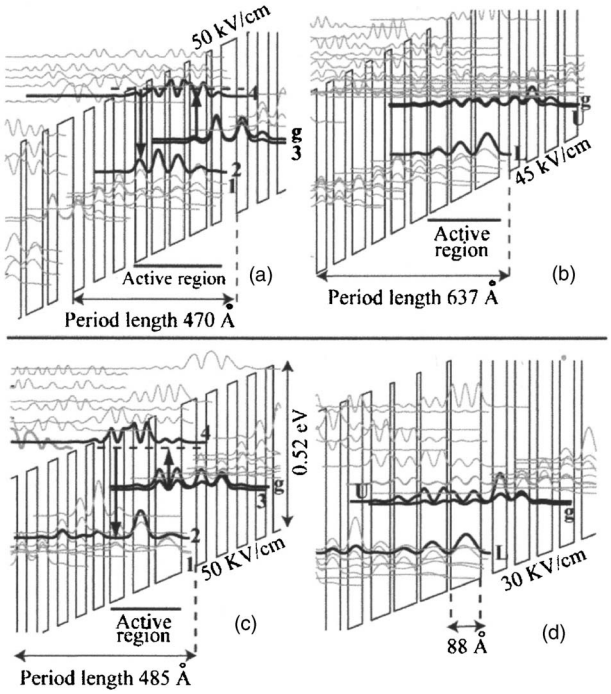

FIG. 1. (a) and (b) Conduction-band diagrams of the nonlinear (a) and pump (b) regions, respectively, in Wafer D3015. The barrier/well widths of each of the 26 periods of the nonlinear stack, henceforth expressed in nanometers, are 4.5/**3.1**/2.9/**3.1**/2.5/**3.2**/3.0/**3.3**/1.5/**3.7**/1.5/**4.2**/1.5/**4.8**/1.5/**2.7**, where the wells are shown in bold face, and the barriers in plain face. The underlined layers are doped to 2×10^{17} cm^{-3}. The optical dipole matrix elements involved in the AS–Raman transition are $z_{43}=1.8$ nm and $z_{42}=2.0$ nm. The pump laser is a conventional 20-stage QC stack emitting at $\lambda\sim8.3$ μm. (c) and (d) Diagram of the conduction band of the nonlinear region (c) and pump region (d), respectively, in Wafer D2924. The pump is a conventional 30-period QC-laser emitting at $\lambda\sim10.5$ μm. The layer thicknesses of each of the 30 periods comprised in the nonlinear stack are 4.0/**2.6**/2.9/**2.9**/2.6/**2.7**/2.3/**2.7**/2.0/**2.7**/1.7/**3.8**/2.5/**4.2**/1.8/**7.1**, following the same notation as above. The doping concentration in the underlined wells/barriers is 2×10^{17} cm^{-3}. The optical dipole matrix elements z_{43} and z_{42} are estimated to be 1.8 nm and 0.6 nm, respectively. In all cases, the InGaAs wells and AlInAs barriers are grown lattice matched to the InP substrate. The moduli squared of the relevant wavefunctions are also shown. In (a) and (c), the black arrows indicate the Raman transition and the levels involved are numbered. In (b) and (d), the letters U and L indicate the upper and lower pump laser levels, respectively. The ground level of the injector is labeled as g in all four plots.

gion. The waveguide specifications, including both layer thicknesses and doping concentrations, change slightly from one design to another. However, absorption coefficients and confinement factors are optimized toward low loss and high optical confinement and are very similar for the different wafers.

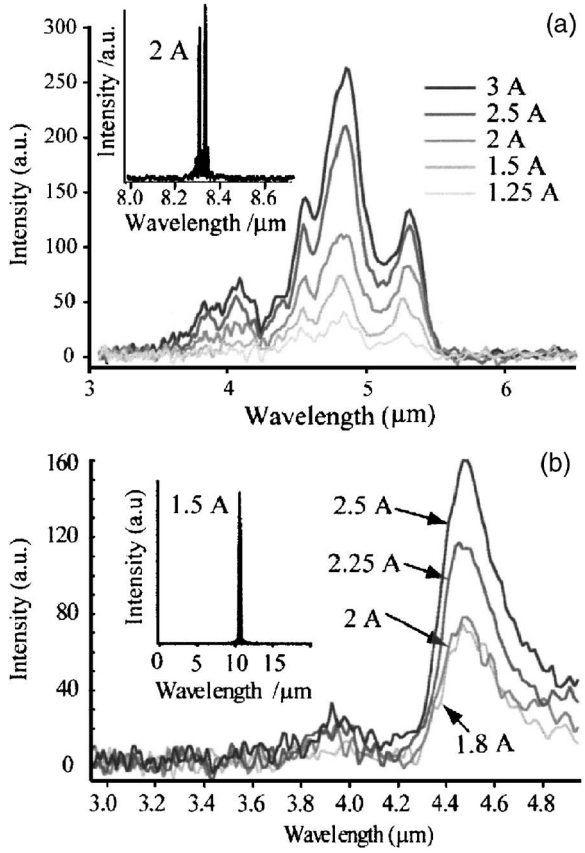

FIG. 3. (a) Short-wavelength emission spectra of D3015 above laser threshold. Peaks attributed to AS–Raman emission (4.8 μm) and incoherent upconversion (5.3 μm) can be distinguished. The dip observed around 4.3 μm is characteristic of CO_2 absorption. The inset shows the spectrum of the pump laser measured at a heat sink temperature of ~90 K and 2 A peak current. (b) Short-wavelength luminescence spectra, above threshold, of D2924 measured near liquid-helium temperatures (~7 K). The main peak at 4.5 μm is attributed to AS–Raman emission. The inset shows the pump spectrum measured at ~90 K and a peak current of 1.5 A.

The short-wavelength emission spectra of the samples were measured in pulsed mode (100 ns current pulses and ~80 kHz repetition rate), using a Nicolet 860 Fourier transform infrared spectrometer and a cooled InSb detector.

Figure 3(a) shows the spectra of sample D3015 measured at different peak currents, all above pump laser threshold (1 A, see Fig. 4). The upper inset shows the spectrum of the pump light for a peak current of 2 A. The main peak at

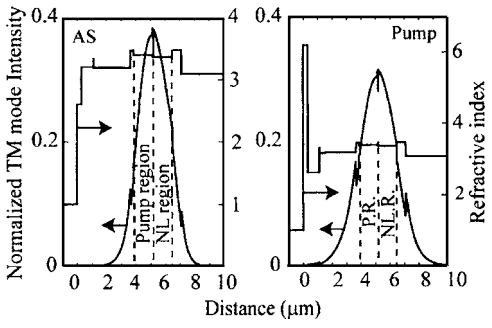

FIG. 2. Normalized mode intensity profile and profile of the real part of the refractive index in the reverse growth direction (the substrate is located on the right-hand in the graphs) for both AS and pump fundamental modes in Wafer D3015.

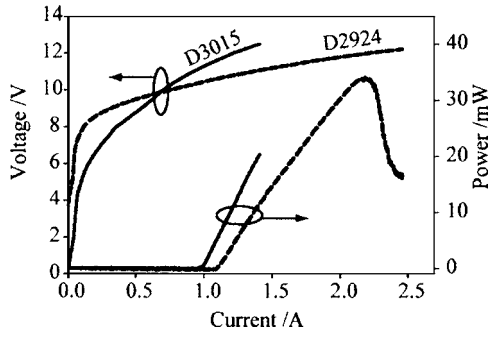

FIG. 4. LIV characteristics of the lasers of wafers D3015 (solid lines) and D2924 (dashed lines). These measurements were carried out at liquid-nitrogen temperatures.

Downloaded 29 Aug 2006 to 128.112.35.48. Redistribution subject to AIP license or copyright, see http://apl.aip.org/apl/copyright.jsp

4.8 μm (258 meV) can be attributed to AS–Raman scattering ($h\nu_{\text{pump}}=150$ meV and $\Delta E_{32}=110$ meV—from luminescence measurements below pump laser threshold—giving an expected $\lambda_{AS}=4.8$ μm ($h\nu_{AS}=260$ meV)). Pumping in sample D3015 is taking place above resonance, and electrons in Level 3 excited by the pump photons can easily scatter into Subband 4, and decay spontaneously into Level 2. Such incoherent upconversion process is the cause of the peak observed at 5.3 μm (235 meV), which is truncated by the wavelength cutoff at $\sim$5.4 μm of the InSb detector. This measured photon energy of 235 meV is larger than expected by design ($\Delta E_{42}=225$ meV). The detuning, obtained from the shift between the lines corresponding to AS–Raman scattering and incoherent upconversion, is $\delta=258$ meV -235 meV$=+23$ meV.

The short-wavelength emission spectra of the sample with negative detuning, D2924, were measured at 7 K for different peak currents (1.8, 2.0, 2.25, and 2.5 A) above the pump laser threshold (1.1 A, see Fig. 4), and are displayed in Fig. 3(b). The main feature is a peak at around 4.5 μm (276 meV), which is attributed to AS-Raman scattering ($h\nu_{\text{pump}}=118$ meV and $\Delta E_{32}=155$ meV—from luminescence measurements below threshold—giving an expected $\lambda_{AS}=4.5$ μm ($h\nu_{AS}=273$ meV)).

In the nonlinear region of D2924, there exist large optical dipole matrix elements for several transitions from Level 4 to lower-energy states other than Level 2. As a result, it is possible to have AS emission at various wavelengths. Such emission is seen from transitions to the state immediately above Level 2 and 145 meV below Level 3 by design, which would give the AS emission at around 4.7 μm, thus explaining the asymmetry of the peak. In addition, the small peak observed at approximately 3.9 μm (318 meV) can be explained by AS emission involving the states labeled as 1, (202 meV and 207 meV below State 3 by design, respectively).

Electrons in State 3 can be excited by the pump light into Level 4 and then decay spontaneously to the lower State 2, emitting a photon of energy ΔE_{42}. However, in this case, we are pumping the nonlinear region well below the subband resonance, with a detuning of $\delta=h\nu_{\text{pump}}-\Delta E_{43}=118$ meV -137 meV$=-19$ meV, which makes the real transfer of electrons to State 4 less likely. Consequently, the spectra in Fig. 3(a) show practically no emission at $\lambda\sim4.2$ μm (corresponding to $\Delta E_{42}\approx137+155$ meV).

Figure 4 shows the light-current-voltage (*LIV*) characteristics of Samples D2924 and D3015. AS–Raman emission is seen at operating voltages of $\sim$13 V for both Samples D2924 and D3015, which agrees well with the value expected from the design electric fields across the various substacks.

In summary, in this letter, we have presented experimental evidence of electronic AS–Raman emission in QC lasers. Such nonlinear light generation was observed in separate samples utilizing distinct nonlinear (and pump laser) active region designs. The frequency shifts between AS–Raman and pump photons were measured to be over 100 meV, significantly larger than those reported with intersubband Stokes–Raman lasers. In addition, all lasers in which the nonlinear region is pumped above resonance with the transition 4-3 were found to emit light via incoherent upconversion processes. In our measurements, no narrowing of the AS emission peak, which would indicate AS–Raman gain in our samples, has been observed so far. However, we believe that further optimization of the nonlinear region, specifically amending the sample design to obtain an optimized (smaller) detuning δ and an increase in the pump power should lead to achieving electronic AS-Raman lasing.

This work was supported by the MRSEC Grant at Princeton University, NSF DMR-0213706. One of the authors (A.G.I.) wishes to thank EPSRC for financial support. Another author (A.B.) acknowledges support from TAMU TITF Initiative.

[1] J. Faist, F. Capasso, D. L. Sivco, C. Sirtori, A. L. Hutchinson, and A. Y. Cho, Science **264**, 553 (1994).
[2] M. K. Gurnick and T. A. DeTemple, IEEE J. Quantum Electron. **19**, 791 (1983).
[3] M. M. Fejer, S. J. B. Yoo, R. L. Byer, A. Harwit, and J. S. Harris, Phys. Rev. Lett. **62**, 1041 (1989).
[4] E. Rosencher, A. Fiore, B. Vinter, V. Berger, P. Bois, and J. Nagle, Science **271**, 168 (1996).
[5] Al. Belyanin, F. Capasso, V. V. Kocharovsky, V. V. Kocharovsky, and M. O. Scully, Phys. Rev. A **63**, 053803 (2001); **65**, 053824 (2002).
[6] N. Owschimikow, C. Gmachl, A. Belyanin, V. Kocharovsky, D. L. Sivco, R. Colombelli, F. Capasso, and A.-Y. Cho, Phys. Rev. Lett. **90**, 043902 (2003).
[7] O. Malis, A. Belyanin, C. Gmachl, D. L. Sivco, M. L. Peabody, A. M. Sergent, and A. Y. Cho, Appl. Phys. Lett. **84**, 2721 (2004).
[8] T. S. Mosely, A. Belyanin, C. Gmachl, D. L. Sivco, M. L. Peabody, and A. Y. Cho, Opt. Express **12**, 2972 (2004).
[9] H. C. Liu, C. Y. Song, Z. R. Wasilewski, A. J. Spring Thorpe, J. C. Cao, C. Dharmawardana, G. C. Aers, D. J. Lockwood, and J. A. Gupta, Phys. Rev. Lett. **90**, 077402 (2003).
[10] M. Troccoli, A. Belyanin, F. Capasso, E. Cubucku, D. L. Sivco, and A. Y. Cho, Nature (London) **433**, 845 (2005).
[11] N. Owschimikow, C. Gmachl, A. Belyanin, V. Kocharovsky, D. L. Sivco, R. Colombelli, F. Capasso, and A. Y. Cho, Phys. Rev. Lett. **90**, 043902 (2003).
[12] C. Gmachl, D. L. Sivco, J. N. Baillargeon, A. L. Hutchinson, F. Capasso, and A. Y. Cho, Appl. Phys. Lett. **79**, 572 (2001).

Downloaded 29 Aug 2006 to 128.112.35.48. Redistribution subject to AIP license or copyright, see http://apl.aip.org/apl/copyright.jsp